

Experimental aspects of dense morphology in copper electrodeposition

V. Fleury, M. Rosso, J.-N. Chazalviel, and B. Sapoval

Laboratoire de Physique de la Matière Condensée, Ecole Polytechnique, 91128 Palaiseau, France

(Received 29 April 1991)

We report an extensive study of electrochemical deposition of copper with growth under galvanostatic conditions and parallel geometry. In such conditions a clear understanding of the origin of the ramified deposit and of its growth speed is possible, at least in the case of dense morphology. We confirm that this morphology belongs to a steady-state regime where growth can be modeled as the displacement of a flat strip of nearly equipotential copper. The growth velocity is exactly the drift velocity of the anions, which is proportional to the current density. We also show that the mass of the deposit does not depend on the speed at which it was grown but only on the concentration of salt in the bulk of the electrolyte. We compute the modifications in concentration profiles and in the electric field due to pH changes during growth.

PACS number(s): 68.70.+w, 82.45.+z, 66.10.Ed, 81.15.Lm

I. INTRODUCTION

Electrochemical deposition of copper and zinc has been widely studied in the past few years [1–11]. These investigations were essentially motivated by the diffusion-limited aggregation (DLA) model [12,13]. In DLA simulations particles are launched at random from a remote source and wander around before sticking to a cluster. The structure of the DLA clusters is fractal.

Electrodeposition of metal from a solution was studied in relation to DLA because of the apparent correspondence between the two problems (as it also occurs with hydrodynamical flows, Saffman-Taylor fingering, and dielectric breakdown, for example); but an important question, which has been little addressed, is the role played by the electrochemical aspects of the problem, which are not taken into account in DLA simulations.

For example, in electrodeposition experiments several morphologies have been reported, among them dense morphology (DM) [2,3], for which a stable envelope grows steadily, and thus does not exhibit a fractal aspect. The physics of the DM regime is then clearly different from DLA [14]. Hereafter, DM is studied for its own purpose since it raises questions on the flux of particles in the vicinity of nontrivial boundaries.

Basically, there are several questions in the case of electrodeposition that may be related to purely electrochemical reactions or dynamics, and not to DLA features. Let us recall some of these questions.

What are the influences of the following? (1) departures from electroneutrality [14], (2) electroconvection and turbulence, (3) electrocapillarity, (4) recrystallization of the deposit, and (5) impurities; one can wonder also (6) what drives the system from fractal regimes to DM regimes [14]. This point is connected to the questions of the distance between the filaments of the deposit [14] and of the branching mechanism. We will attempt in this paper to give a description of the growth in the case of dense morphology in parallel geometry and under constant current conditions. This description will include

the description of departures from electroneutrality and an analysis of the role of impurities. We will first describe the experimental setup and experimental conditions (Sec. II), then the theoretical predictions of the model (Sec. III) and the experimental results (Sec. IV). In Sec. V, we will discuss the morphological transitions that occur at a given fraction of the distance between electrodes (the so-called “Hecker effect”), which are also accompanied with changes in the color of the deposit. Finally, in Sec. VI we will show that a potential drop is found at the tips of the branches, which is compatible with the theoretical prediction of Ref. [14].

II. THE EXPERIMENTAL SETUP

There are two main ways of doing electrochemical experiments that may be related to the DLA paradigm. The first one is to take a solution with a supporting electrolyte, which damps out the electric field and allows the ions to have a motion close to a diffusion-limited one [10,11]. The second one, which has been widely used, consists of adopting a dilute solution without a supporting electrolyte, and applying a large electric field, thus getting close to the DLA numerical equations through the field equations of the electric potential. In that case, the DLA simulation is generally considered as a Monte Carlo simulation of the physical phenomenon. In the following, *electrodeposition* will refer essentially to deposition without a supporting electrolyte, if not otherwise stated.

The electrochemical deposition at the electrodes of a cell has almost always been studied with constant applied voltage, because people intended to mimic the electrochemical analog of the DLA process. When one writes down the ideal electric equations with the electric potential V and the discretized equations of the DLA simulations with the probability P for a random walker of visiting a site outside the deposit, one may indeed think of a one-to-one correspondence.

Electrochemical equations

$$\begin{aligned} \Delta V &= 0 \text{ (Poisson's law)} \\ V_{\Sigma_1} &= 0, V_{\Sigma_2} = V_0 \text{ (potential at the electrodes)} \\ v &\approx -\nabla V \text{ (growth kinetic)} \end{aligned}$$

Corresponding DLA equations

$$\begin{aligned} \Delta P &= 0 \text{ (conservation of probability)} \\ P_{\Sigma_1} &= 0, P_{\Sigma_2} = 1 \text{ (probability on the cluster and on the source)} \\ v &= -D\nabla P \text{ (growth kinetic)} \end{aligned}$$

Unfortunately the formal electric problem is already a drastic oversimplification of the reality since these equations assume local and global electroneutrality. Local departures from electroneutrality, which do not appear in this formal model, do really happen in experiments and, as shown by Chazalviel [14], play a major role in the formation and growth of metal branches from a salt solution.

In our experiments we used a constant current, rather than a constant applied voltage, and a parallel geometry. These conditions are much more suitable for controlling the experiment, since one knows exactly what is the rate at which copper is deposited (when working with a constant potential one does not even control the mass deposition rate). Moreover, there is no *a priori* reason for the systematic use of constant voltage when studying DM, which is clearly not fractal on the macroscopic scale, and for which DLA justifications seem poorly relevant.

Circular geometry, with a point cathode and a ring anode, is also broadly used because it enables one to eliminate an otherwise unavoidable scale length: the width of the cell. Sometimes, circular geometry is also stated to provide isotropic conditions. Unfortunately this geometry brings in several experimental problems. It involves a complicated dependence of the growth speed on the radius of the deposit, because the growth is never in a steady-state regime. Also, the circular geometry makes quite uncertain the measurement of growth parameters during the first stage of growth, when the growth rate is actually the largest. The parallel geometry, provided that the cell is several times wider than the width of a typical treelike deposit (in our experiments this ratio was ranging between 20 and sometimes 100), can be profitably combined with constant applied current, for in these conditions the potential difference between electrodes and the growth speed both have a very simple linear behavior as functions of relevant parameters such as time, concentration, or cell thickness, as we shall show in the following.

The experiment therefore consists of growing copper deposits without a supporting electrolyte, between a cathode and a dissolving anode, in pseudo-two-dimensional rectangular cells (see Fig. 1) and with a constant applied current. Our samples consist of two parallel sheet copper blades, separated by a distance of 2 cm, that are pressed between two glass plates. This cell is filled through the open sides. Unlike other experiments, our glass plates are not stuck to each other, but rather they are held tightly together with a special device (see Fig. 2) that permits very good parallel alignment of the plates. This system allows rapid rinsing of the samples, and the use of the same electrodes for many experiments. Especially, electrodes that exhibited systematic anomalous growth, attributed to surface imperfections, could immediately be repolished, or discarded. The growth is

filmed with a television camera, recorded and digitized with standard programs software and hardware. In the experiments that we report on here, the thickness of the cell could be chosen in the set 0.05, 0.1, 0.15, 0.2, and 0.3 mm. The concentration of copper sulfate ranged between 0.005 and 0.1 mol ℓ^{-1} . The distance between the two electrodes could also be varied. The constant values of the current could be fixed between 0.1 mA and nearly 30 mA.

A number of practical problems caused limitations on the use of the different ranges of parameters. The most obvious and frequent of them was the formation of bubbles at the cathode and within the deposit that prevented one from imposing very high current densities through the cell. That is to say that currents as high as 20 mA, though easily achieved, could not be applied to the thinner cells or less concentrated solutions since it would not have resulted in the growth of a DM deposit but merely in the formation of a mess of bubbles, due to both hydrogen evolution and electroconvection, which break the growing trees.

For very-low-current densities the deposits are no longer dense and form patterns similar to the ones obtained for low constant potentials that have already been reported by several authors [1–10]. There is, however, a difficulty in defining the critical current density, if any, at which the change occurs. As the current density decreases the envelope of the tips and the branches themselves both become increasingly tortuous, but sometimes the envelopes already show oscillations or instabilities while the branches still seem rectilinear. We had to choose an empirical criterion for defining a so-called stable envelope. We considered DM fronts, ones with parallel branches advancing altogether, so that the distances between tips remained smaller than 1mm. Since

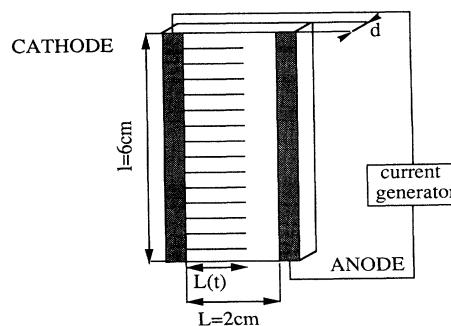


FIG. 1. A typical rectangular cell. Studied thicknesses: 0.05, 0.1, 0.15, 0.2, and 0.3 mm. The same electrodes were used for many experiments. The electrodes are pressed between two glass plates, thus forming a cell.

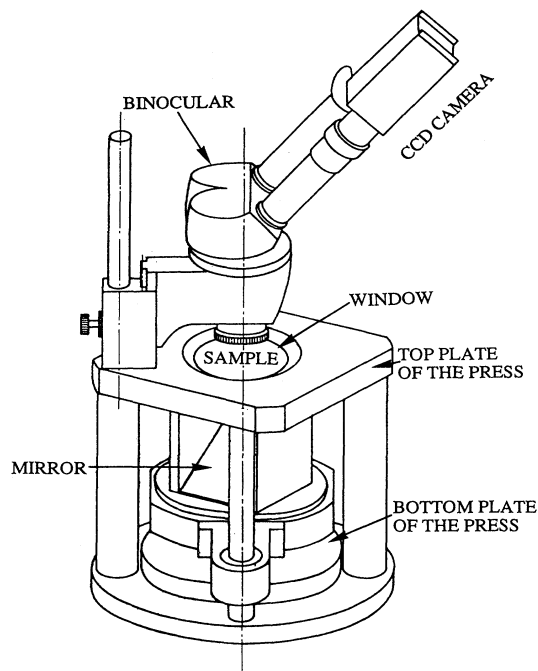


FIG. 2. The experimental device. The sketch does not show the video and the computers to which the charge-coupled-device (CCD) camera is connected. The cell is pressed between two thick plastic plates. The growth is observed through a circular window, while it is lit from the side with the help of a mirror, which is borne by the sample holder. A vertical screw lifts the sample holder and presses it against the circular window so that the parallelism is almost perfect, though the change of sample can be done very quickly. This device allows rapid rinsing of the cell, and the use of the same electrodes for many experiments.

the transition between fractal regimes and dense regimes is smooth, one can hardly speak of a "phase diagram"; however, the current density seems the right tunable parameter and not the potential difference. So, previously reported phase diagrams [2,3], which seem very complicated in a potential-concentration plot, may be understandable in terms of current density.

III. EXPECTED FEATURES AND THEORETICAL PREDICTIONS

Numerical and analytical work on parallel electrodeposition has been reported by Chazalviel [14], and some preliminary experimental results have appeared in a short communication [15]. We recall here the most important conclusions of these papers.

First of all, it is well known that when setting an electric field between the electrodes the anions move towards the anode and the cations towards the cathode, with a drift velocity equal to their mobility times the electric field. As a consequence cations are discharged and deposited at the cathode, and in the absence of stirring, anions migrate and pile up near the anode. Cations are formed at the anode. Therefore, the situation is not

symmetrical. It comes out from numerical and analytical work [14] that, if the deposit were compact, the collective motion of the cations and of the anions, that have to follow the electric force, would result in an anion-depleted zone near the cathode. This is not so because the system cannot withstand the huge electric field that would appear in the vicinity of the cathode. Instead, branches start forming and growing. The simple result is that, at any time, this motion hinders or limits the formation of this depleted zone. In order for this compensation to be efficient at every moment, the growth speed of the deposit must then be equal to the speed at which the charged zone tries to form, which is the speed at which anions withdraw. The profile of concentrations should be the following (Fig. 3): The zone invaded by the branches should be almost free of ions of any kind, because of deposition of copper and drifting out of the anions, and in the zone between the tips and the anode the concentration should be constant for both kinds of ions, since ahead of the branches two fluxes of ions simply cross each other neutrally in opposite directions. A thin layer due to the piling up of anions, and hence accumulation of a part of the copper cations produced by the dissolving anode, should be formed at the anode.

If these statements are correct, then the main part of the potential drop through the cell is caused by the shrinking of the zone comprised between the tips and the

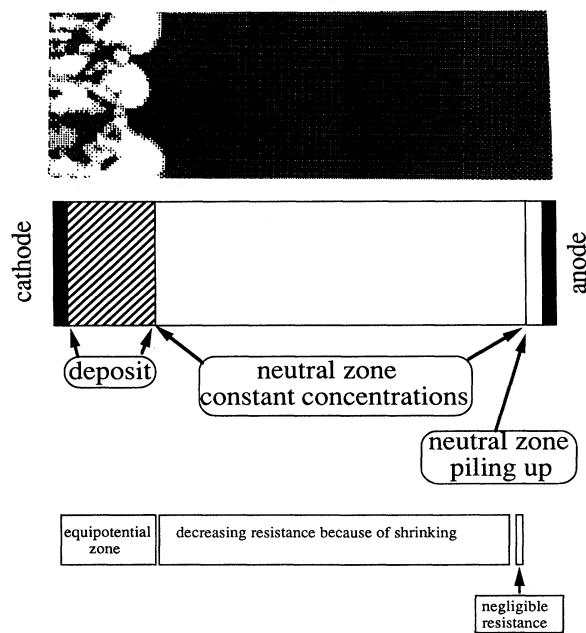


FIG. 3. The profile of concentration and the corresponding electrical regimes. The upper image comes from a real experiment performed with a colored salt of copper, namely, $\text{Cu(II)-Naphthol-blue-black}$. The shaded area ahead of the deposit has a constant color, while the zone between the branches of the deposit becomes transparent: this indicates that the anions have drifted out. This migration strictly follows the growth of the deposit. A thin darker layer forms at the anode, thus confirming the predicted piling up.

anode. The progressive shrinking causes a proportional increase of the conductance of the cell. The thin layer at the anode participates very little in the resistivity of the cell, because it is much thinner than the main part of the cell and much more concentrated, therefore it behaves like a small resistance put in series with a much larger one. More quantitatively the width over which this thin layer extends is of order \sqrt{Dt} (in which D is the diffusion constant and t the time), which is smaller than 1 mm in our experiments. When the deposit has reached the fraction f of the size L_0 of the cell, the zone ahead of the tips is composed of a length $L_0(1-f)$ of a solution that is identical to the initial one, and of a second layer, 1 mm thick, whose concentration is of the order of ten times larger than the initial concentration, which is quasineutral. The latter zone is then roughly ten times thinner and ten times more concentrated than the initial solution; its resistance is then of the order of a hundred times smaller. Of course these arguments break down when the deposit is very close to the anode, when the neutral zone is negligible ($f=1$). It also breaks down for very long times since in this case the diffusion spreads a large fraction of the ions far away in the solution. A detailed study of the roles of diffusion driven motion and electrically driven motion is also of great importance in order to understand the origin of the shape of the deposit. This study is done in Ref. [14]. The equations of the moving interface must be derived by taking into account the different zones that are found in the cell during growth. These equations are merely obtained by repeatedly applying Ohm's law with the upper assumptions. (The analog equations for a circular geometry were independently presented [9(b)] by Melrose and Hibbert.)

Let us call V the potential, E the electric field, v the speed of the front, I the applied current, J the current density, $L(t)$ the position of the deposit at time t , S the transverse area of the cell, μ the mobility of an ion, and Δ the potential drop found at the growing tips of the deposit (this quantity is assumed to be a constant in the steady-state regime, but can be different for different experimental conditions).

The subscript a stands everywhere for anion, and the subscript c stands for cation (here copper); then

$$I = (C_c z_c \mu_c e + C_a z_a \mu_a e) E S, \quad (1)$$

$$V_{\text{anode}} - V_{\text{cathode}} = \Delta + R(t) I, \quad (2)$$

in which

$$R(t) = \frac{L(t)}{Se(C_c z_c \mu_c + C_a z_a \mu_a)}$$

is the equivalent resistance of the solution between the tips and the anode when neglecting the thin layer of more concentrated solution that forms near the anode.

Let us emphasize the following point: one would expect the concentrations that enter the formulas to depend on time; clearly, if all the anions are repelled by the advancing front, then the anions are always located between the tips of the branches and the anodes and, if the tips move toward the anode, the concentration ahead of the branches increases while the volume comprised between

the branches and the anode decreases. However, it is true that *average* concentrations increase, but this average is taken over two zones: namely, the Ohmic zone where the concentrations remain identical to the ones at $t=0$, and the very thin layer where ions pile up, and which is not taken into account in the calculation of the resistance of the solution, as it has already been shown. This is why the concentrations in (1) and (2) remain constant.

The growth speed is simply related to the field by the anion mobility

$$v = \mu_a E, \quad (3)$$

$$E = \frac{I}{Se(C_c z_c \mu_c + C_a z_a \mu_a)}. \quad (4)$$

Given these relations one can easily compute the different relevant parameters as functions of the applied current, which is the control parameter we have chosen (simple geometrical factors relate the field to the current),

$$v = \frac{I \mu_a}{Se(C_c z_c \mu_c + C_a z_a \mu_a)}, \quad (5)$$

$$V_{\text{anode}} - V_{\text{cathode}} = \Delta + \frac{L(t) I}{Se(C_c z_c \mu_c + C_a z_a \mu_a)}, \quad (6)$$

$$L(t) = L_0 - vt.$$

Rewriting (5) and (6) as they stand in the case of copper sulfate, we get

$$v = \frac{I}{2SeC(1 + \mu_c/\mu_a)}, \quad (5')$$

$$V_{\text{anode}} - V_{\text{cathode}} = \Delta + V_0 - \frac{1}{\mu_a [2SeC(1 + \mu_c/\mu_a)]^2} I^2 t. \quad (6')$$

Using the same kind of algebra, one can compute the ratio Π of the copper in the branches over the copper that was formerly in the solution behind the branches, and one then finds

$$\Pi = \frac{\frac{1}{z_c e} \int_{t_0}^t dQ}{C_c L(t) s} = \frac{C_c z_c \mu_c + C_a z_a \mu_a}{z_c C_c \mu_a}, \quad (7)$$

$$\Pi = 1 + \mu_c/\mu_a.$$

Taking the following standard values from data books, $\mu_c = 5.76 \times 10^{-4} \text{ cm}^2 \text{ v}^{-1} \text{ s}^{-1}$ and $\mu_a = 8.64 \times 10^{-4} \text{ cm}^2 \text{ v}^{-1} \text{ s}^{-1}$, we find that Π should be 1.66 at 25°C. It may seem surprising that the ratio of the copper deposited in the branches over the copper that was formerly in the solution in the area invaded by the branches should not be exactly one, and that it does not depend on the speed at which the deposit is grown (a nonconstant speed will even give the same result). One can naturally wonder where the "supplementary" copper comes from. One must realize that the situation is not static, the copper in the deposit comes from two contributions. These two contributions clearly appear in (7) as two terms which

represent the two components of the current. The existence of two parts in the current can be explained in two different but complementary ways: first, one can remain in the laboratory frame and say that the current is composed of a cationic current plus an anionic current. This anionic component is surprising since the anions do not deposit. However, the anions migrate and pile up at the anode, hence carrying a part of the current. Second, one can go in the moving frame of the advancing front, thus canceling the anionic current. In this case, the interpretation is that one must add to the speed of the cations the speed of the moving frame, which is precisely the speed of the anions. This situation is not usual in electrochemistry, where the solution is generally stirred in order to prevent the formation of concentration gradients. The result on the amount of copper present in the branches is quite enlightening, since it shows that this mass does not depend on how fast the deposit is grown. This is to say that for a given concentration, the linear density of the deposit is the same, whatever the growth speed. As a consequence, the ratio of the linear densities of two filaments grown at different speeds is equal to the inverse of the ratio of the number of branches in the deposit.

The geometrical factors that enter the current density and the electric field imply that the growth speed should be constant throughout the cell [Eqs. (3) and (4)] for a fixed current density. Concerning the potential difference between the electrodes, one notices that V varies linearly with time [Eq. (6)]. dV/dt is constant during the growth, and related to growth speed by an $I/(2SeC\Pi\mu_a)$ factor [Eqs. (5) and (6)]. The growth speed should vary linearly with the applied current [Eqs. (5) and (5')] and dv/dI should be proportional to $1/C$. Some of the main aspects of the growth presented here were first and briefly issued in Ref.[15].

IV. EXPERIMENTAL RESULTS

We now give the experimental results and explain some of the experimental limitations.

A. The potential drop

The potential drop between the electrodes for a given current, a given cell thickness, and concentration was measured. A typical curve is shown in Fig. 4. Three regimes, in fact, can be distinguished. First a transient regime at the early stages characterized by an overshoot of a few volts. This period corresponds to the delay that is needed before building up the first "trees" and the steady-state envelope. This delay only depends on the current density, and does not depend, for example, on the distance between electrodes. As a matter of fact, as soon as one uses a parallel geometry and a constant current density, the growth is in the same steady-state regime, whatever the distance between electrodes (note that this is at variance with the commonly used circular geometry).

Next, one finds a linear regime that lasts until the branches arrive at a couple of millimeters from the anode and stop growing. The only effect of increasing the distance between electrodes is to make this steady-state re-

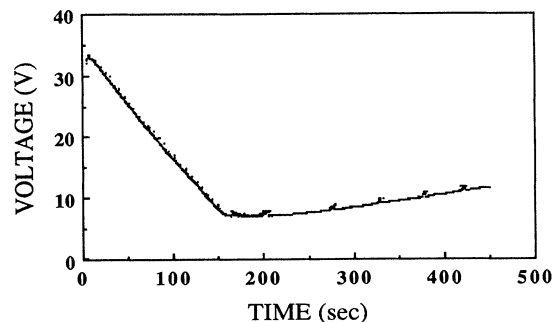


FIG. 4. The potential difference between anode and cathode vs time plot. The voltage vs time curve exhibits three main regimes. The building up of a potential drop takes less than 10 sec. Afterwards, the linear region corresponds to the growing dense parallel morphology. The increase of the potential that is observed after 175 sec corresponds to the noisy regime that starts when branches arrive in the vicinity of the anode. Experimental conditions are as follows: current of 10 mA, thickness of 0.2 mm, concentration 10^{-2} mol ℓ^{-1} .

gime proportionally longer.

At the end, there is a noisy regime where the copper is no longer deposited on thin branches but rather on "blossoming cauliflower florets" very close to the anode and facing it. This regime is accompanied by a huge increase of the cell resistance, and lasts until bubbles appear [in the case of "fractal" growths, the general outlook of the $V(t)$ curve is the same as above, showing that this kind of measurement is only sensitive to the average of the potential]. The experimental measurements that we report in this paper were done after the overshoot, during the linear regime, which starts generally a few seconds after the beginning of the growth and lasts in most cases until the arrival in the vicinity of the anode.

B. The growth speed

The linear regime for the potential decrease takes place at the same time as the linear regime for the growth speed. In this regime, the growth speed was found to be almost constant. (Fig. 5), as long as the deposit is of the same morphology (see Sec. V). The only errors arose from the definition of a stable envelope. In the range of parameters for which the stability was not found to be perfect, we averaged over several runs in order to get better accuracy. The dependence of growth speed on current was extensively studied, and it was found to be linear in the range of parameters studied (Fig. 6), as expected. The variation of growth speed with concentration was also studied. Figure 7 shows $dv(I)/dI$ as a function of $1/C$. The agreement with the predicted curve is fair. We wish to mention that this curve required hundreds of runs and is very reliable.

Several authors (Ref. [4] and references therein) working in circular geometry found a constant growth speed, varying linearly with V , the applied potential. We must stress the fact that working in circular geometry and constant potential, and assuming the same hypotheses as the ones we present in this paper for the linear regime, imply

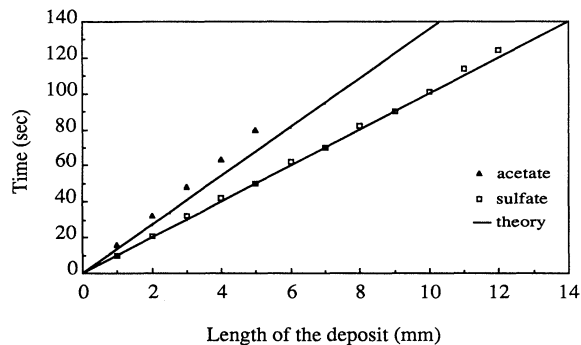


FIG. 5. The grown length vs time for copper sulfate (top) and copper acetate (bottom). The straight lines show the theoretical predictions, which are in fair agreement with experiment. The conditions are concentration, 10^{-2} mol ℓ^{-1} , and spacing, 0.1 mm.

that the growth speed during one growth should vary like

$$V/(R \ln R) \quad (8)$$

(see also Ref. [5] and Fig. 8), where R is the radius of the growing deposit.

It is then normal to find a linear dependence in V , as they observed (but could not explain). However, as noted by the authors it is not so normal to find a constant speed

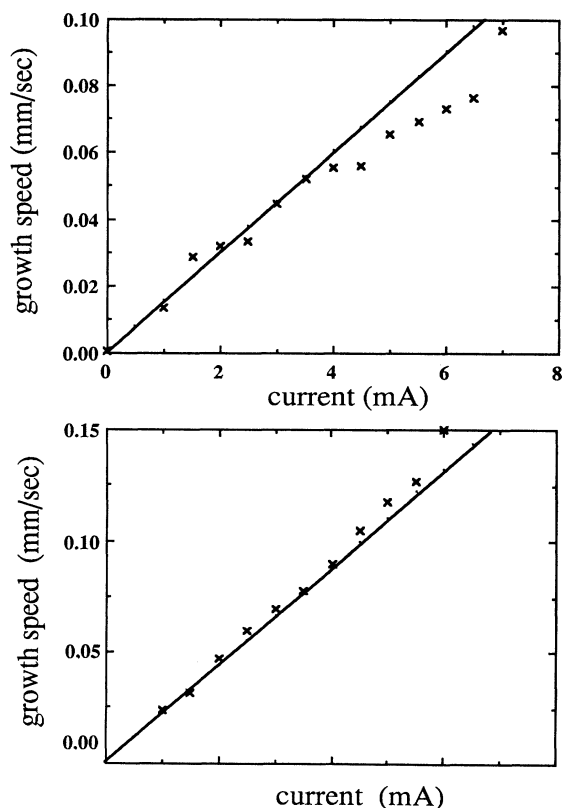


FIG. 6. Growth speed vs applied current for copper acetate 10^{-2} mol ℓ^{-1} (up) and copper sulfate 10^{-2} mol ℓ^{-1} (down). The straight line is the theoretical prediction.

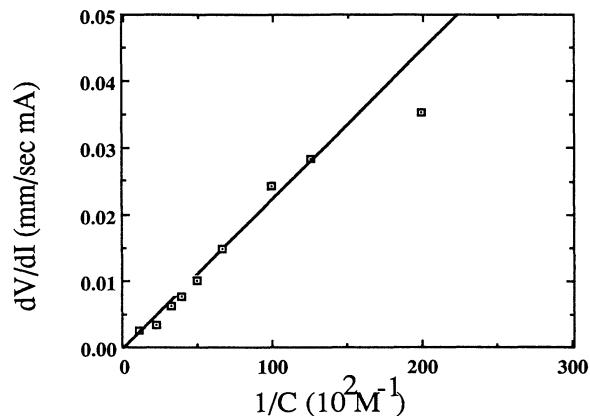


FIG. 7. The behavior of dv/dI as a function of $1/C$. A departure from rectilinearity is noticed for the higher currents. The straight line is the theoretical prediction: the agreement is excellent. Growth speeds are in millimeters per second, concentrations are in 10^{-2} mol ℓ^{-1} units, and currents in milliamperes. The thickness of the cell is 0.2 mm.

throughout the cell. Actually, the reason why the growth speed could have been found to be almost constant in circular geometry (growth speed should be constant only in parallel geometry), might be that the speed profile [Eq. (8)] is indeed very flat (Fig. 8), except very near the electrodes of the cell. Also, in circular geometry, the front perimeter increases during growth. In particular, the measurement of the speed of the front is not easy when the front perimeter is still small, which corresponds to the region where the largest variation of the speed could be expected, according to Eq. (8) and Fig. 8.

C. The dependence on thickness

Since growth speed and $dV(t)/dt$ are just proportional within a factor $\rho I/S$ (where ρ is the resistivity of the electrolyte), we have performed a systematic investigation of $dV(t)/dt$ as a function of current and cell thickness. We have plotted in Fig. 9 $dV(t)/dt$ as a function of the current density, for different thicknesses: 0.05, 0.1, 0.15, and 0.2 mm. The curve is the theoretical prediction when taking into account the effect of nonideally dilute solution on the mobility values [16] ("finite dilution effect"): the agreement is excellent.

D. The copper ratio

The assumptions made in this paper imply that the ratio of copper deposited to the copper that was formerly in the zone invaded by the branches should be $1 + \mu_c/\mu_a$. The copper deposited is measured as

$$\frac{1}{z_c e} \int_{t_0}^{t_1} \frac{dQ}{dt} dt, \quad (9)$$

where t_0 is the time at which branches start forming,

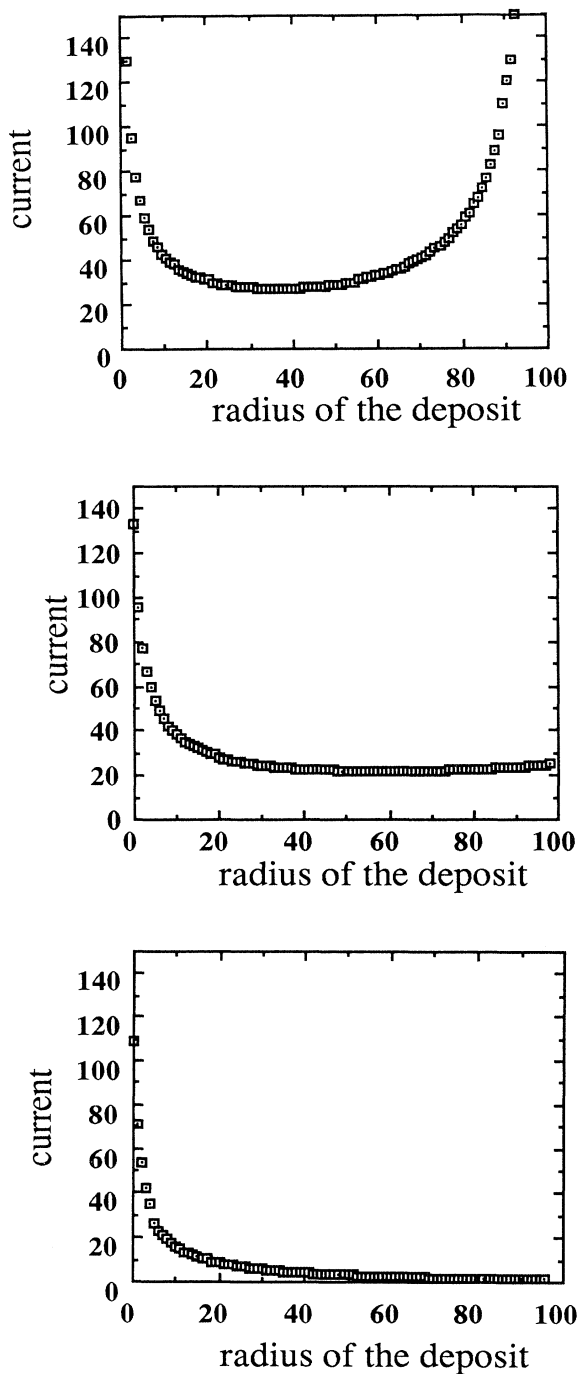


FIG. 8. The three plots show the dependence of the current density and hence the speed at the edge of a flat advancing disk vs the radius of the disk (a value of 100 corresponds to the arrival at $R = R_{\text{anode}}$). The current is in arbitrary units. The plots are given for different ratios of the effective resistivity of the disk over the resistivity of the remaining solution between the disk and the anode. From top to bottom the ratio is 0, 1/100, 1/10. Note that the profile is flatter when the resistivity of the copper deposit is larger. The largest variations of the current should be expected at the beginning and at the end of the growth, where either the growth speed is difficult to measure or the deposit enters a three-dimensional regime.

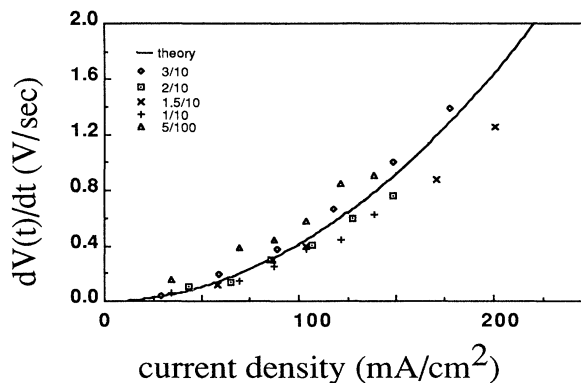


FIG. 9. In the linear regime dV/dt is constant. This quantity is predicted to behave as the square power of I and as the inverse of the square of the thickness of the cell (see the formula in the text). We have then plotted the quantity (dV/dt) as a function of the current density for different cell spacings. The thicknesses are expressed in millimeters.

after the potential overshoot. On the other hand, the copper in the area invaded by the deposit is $CL(t)ld$, where C is the concentration, $L(t)$ the location of the advancing front, and l the width of the cell. The ratio is then easy to compute. The results are shown in Fig. 10 for some currents, spacings, and concentrations. There is a fair agreement with the predicted value (1.66), the experimental value lying between 1.6 and 2.4 depending on the concentration used. For a concentration of $0.01 \text{ mol } \ell^{-1}$ of copper sulfate, the experimental value of the copper ratio is very close to its theoretical value (1.66), derived for infinitely dilute solutions; for other experimental conditions the value of the copper ratio is not so close to 1.66; this will be commented on in Sec. IV F and in Sec. V.

E. Effect of changing the anion mobility

There is still another quantity that can be experimentally modified: the mobility of the anion. We did with copper acetate the same experiments that we had done with copper sulfate. Some features are actually different, described as follows:

- The front is more unstable even though branches are filamentary.
- Bubbles occur very easily and they often hinder the growth.
- The DM pattern often looks like a group of branches with the same root growing like an open fan, instead of looking like gently parallel branches with translational invariance.
- The Hecker effect is much more visible.

In the case of copper acetate the diffusion coefficient at 25°C taken from standard data books is $1.09 \times 10^{-5} \text{ cm}^2 \text{ s}^{-1}$ and the charge is one, then the ratio Π should equal 2.33.

The general behavior in the case of electrodeposition of

copper acetate is the same as for copper sulfate: growth at a constant speed (Fig. 5) with a linear dependence of growth speed with current density (Fig. 6). The experimental data for the copper ratio are in qualitative agreement with the prediction (Fig. 11); however, the experiments show a departure from the value expected from standard data since we found the experimental values between 2.3 and 3.5 for several concentrations. Moreover, the copper ratio was found to increase slightly with the applied current, which had not been so neatly observed in the case of copper sulfate. This, again, will be commented on in Sec. IV F and in Sec. VI.

F. The dependence on concentration

It has been reported [5] that the growth speed seemed not to depend on the concentration and that the system

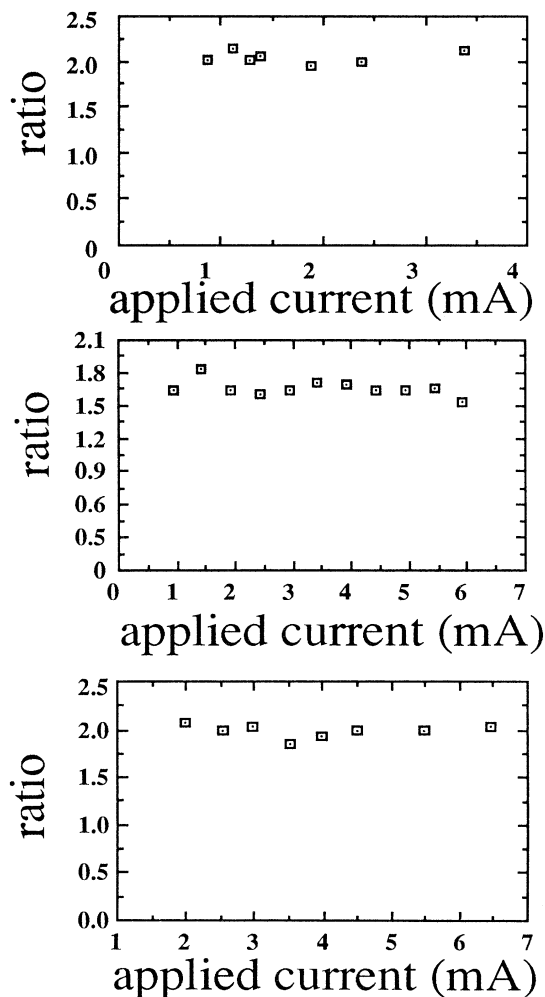


FIG. 10. The ratio Π of the copper deposited in the branches over the copper that was formerly in the zone invaded by the branches is shown for copper sulfate, for some experimental conditions. The thickness is always 0.2 mm, the concentrations are $10^{-2} \text{ mol } \ell^{-1}$, $10^{-1} \text{ mol } \ell^{-1}$, $5 \times 10^{-3} \text{ mol } \ell^{-1}$.

selects the branching rate, or the compaction of the branches, in order to adjust the speed. There is indeed nothing surprising in this: one should notice that, when working with constant potential, the electric field is always the potential difference divided by the distance between the opposite ends of the cell (or between the front of the deposit and the anode); hence this field does not depend on salt concentration (neither the potential difference nor the geometry of the cell depend on concentration); since the speed is proportional to the field, we conclude that the growth speed, when growth is achieved

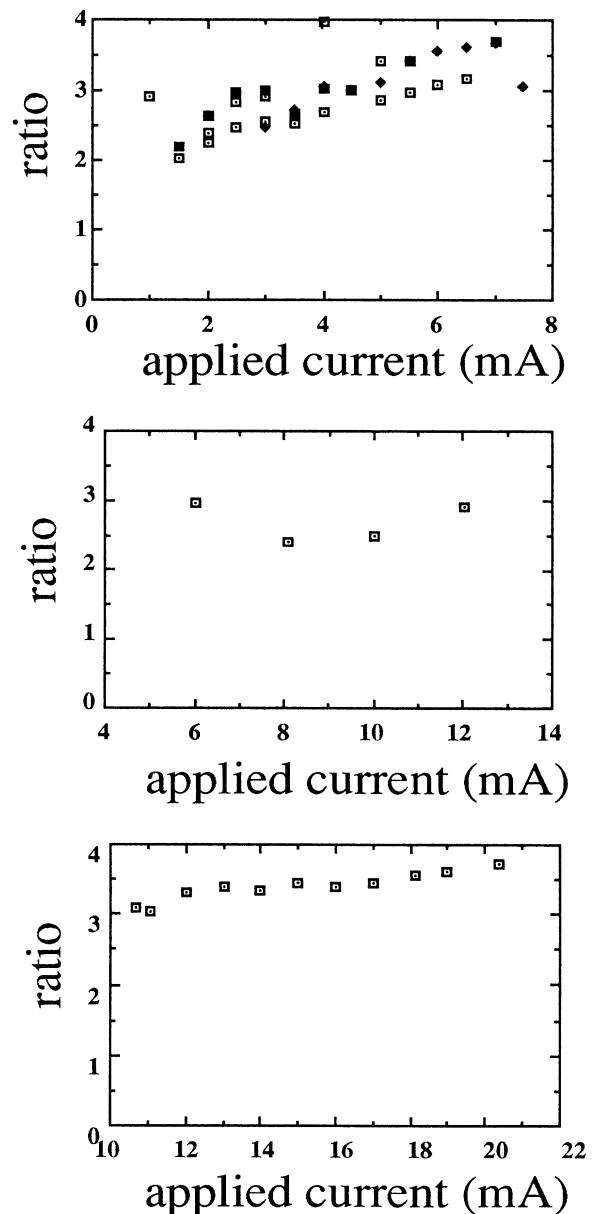


FIG. 11. Same as in Fig. 10, for copper acetate. The concentrations shown are $10^{-1} \text{ mol } \ell^{-1}$, $10^{-2} \text{ mol } \ell^{-1}$, and $2.5 \times 10^{-2} \text{ mol } \ell^{-1}$.

with constant potential, indeed does not depend on concentration. Of course, since the concentration has an influence on the mobility [16], one must expect a slight increase of the growth speed for the larger concentrations when the solution is very far from an ideal dilute solution. One can try to include a full treatment of the dependence of the mobility on concentration.

The dependence of the ion mobility on the concentration comes from two different effects [16]: First, the electrophoretic effects on the ionic cloud that surrounds and screens the ionic charge and, second, the relaxation component of the drift velocity [16]. These well-known effects give rise to a dependence of the mobility on the reciprocal Debye-Hückel length χ

$$\chi = \left[\frac{1}{\epsilon k T} (C_a z_a^2 + C_c z_c^2) e^2 \right]^{1/2}$$

(ϵ is the permittivity, k the Boltzman constant) which is

$$\mu(C) = \mu - \frac{ze\chi}{6\pi\eta} - \frac{\mu e^2 \chi \omega}{24\pi\epsilon k T}.$$

The dimensionless factor ω was computed by Onsager, its value is $\frac{1}{2}$ when $z_a = z_c$. (In the expression of the mobility one recovers the empirical law of Kohlrausch, who had found that the mobility behaves as \sqrt{C} .) The expression of μ is useful when comparing the experimental results for $V(t)$ to the theoretical expectation at infinite dilution, since it explains the discrepancy between the two curves.

However, if we write the copper ratio as a function of concentration

$$\Pi = 1 + \frac{\mu_c - \frac{ze\chi}{6\pi\eta} - \frac{\mu_c e^2 \chi \omega}{24\pi\epsilon k T}}{\mu_a - \frac{ze\chi}{6\pi\eta} - \frac{\mu_a e^2 \chi \omega}{24\pi\epsilon k T}},$$

we find, in the case of copper sulfate,

$$\Pi = \frac{5.7 - 2.17\sqrt{C}}{8.6 - 2.71\sqrt{C}},$$

in which the concentrations are expressed in $10^{-2} \text{ mol } \ell^{-1}$.

This expression is a decreasing function of the concentration, while experimentally we have found larger values of the copper ratio. As a consequence, we cannot ascribe the discrepancy between the observed value of Π and the value at infinite dilution to a finite dilution effect. On the other hand, there is evidence of a slight increase of the value of the copper ratio with an increase of the applied current, which can certainly not be ascribed to finite dilution effects. We will show in Sec. V that protons, which are known to be produced at the anode and then migrate in the bulk, are responsible for the unexpectedly large value of Π . Especially in the case of copper acetate, the copper ratio is seen to increase with the applied current: if the value of the copper ratio is extrapolated to the origin (zero current) we see that we recover a value much closer to the expected value; we also attribute this behavior to hydrogen evolution. Indeed, if the anode produces hydrogen, and if hydrogen is incorporated into the depos-

it either as interstitial hydrogen or in bubbles (which is very often the case), then the value of the deposited copper, which we have considered to be given by It/ze , is clearly overestimated, since part of the current will be consumed by proton reduction. The role of the protons will be discussed in greater detail in Sec. V.

G. A direct measurement of ionic mobilities

We wish to underline the interesting fact that, except for a possible role of the protons, the experiments that we report here provide a way of measuring the mobility of both species in the solution. Indeed, if one measures the copper ratio Π , and $dV(t)/dt (=p)$, then the mobilities are given by

$$\mu_a = \frac{I^2}{2SeC\Pi^2 p}, \quad \mu_c = \frac{(\Pi - 1)I^2}{2SeC\Pi^2 p}.$$

V. TRANSITION ZONES

Transitions in morphology are very frequent in DM (but are also observed in fractal regimes [17]). The so-called Hecker transitions scale with the size of the cell, as it has already been reported [5,6,9,15]. In our samples, there were generally two main visible changes in morphology, separating three different zones, each one of a length roughly equal to one-fourth of the deposit length at the end of the growth (sometimes these zones can hardly be noticed unless one knows in advance where indeed to expect a transition zone). Figure 12 shows that the transition can be responsible for a slight change in the variation of the potential drop. For this reason, only the measurements of potential differences before the Hecker transition have been considered when plotting $dV(t)/dt$ as a function of current density.

Some authors claim that morphological changes are some kind of statistical phenomena, reflecting a macroscopic effect of the boundary conditions [19]. Numerical attempts to generate sharp transition lines by growing clusters with biased random walks fail to reproduce the features of the Hecker effect, without even mentioning the rather artificial way of including a bias in the deposition mechanism. We have presented in Ref. [18] a study of the Hecker effect, in which we show that the transition zones are merely due to the migration of ions (copper, sulfate, and impurities) of opposite signs in opposite directions. A similar conclusion has been independently reached by Melrose, Hibbert, and Ball [9(b)]. As shown in Refs. [9(b)] and [18], if a step in the concentration of a given impurity migrates in the solution towards the deposit, one must expect a morphological transition somewhere in between the electrodes, at the place where the impurity front meets the growing deposit. Furthermore, if a non-negligible quantity of protons (for example) is produced at the anode, then it will affect the production of cations, thus altering the supposed steady-state concentrations in the bulk. We now show how the effect of a production of a positively charged impurity, such as protons, will affect the description of the growth.

We suppose that at the start of the experiment the con-

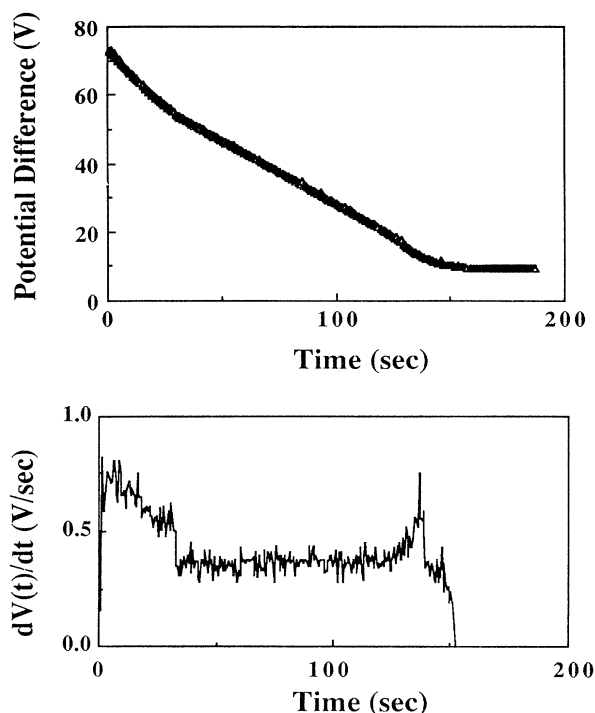


FIG. 12. Top: potential difference $V(t)$ between electrodes during growth, in the case of a fairly neat Hecker effect (copper sulfate $2 \times 10^{-2} \text{ mol } \ell^{-1}$, geometry $6 \text{ cm} \times 2 \text{ cm} \times 0.2 \text{ mm}$, 10 mA). Bottom: derivative $dV(t)/dt$, in this case the change of slope is of the order of 25%, leading to a value of C_{H}^* of the order of $10^{-2} \text{ mol } \ell^{-1}$.

centrations of anion and of metallic cation are C_a and C_c , and that the concentration of protons is negligible (a concentration C_{H} of protons could easily be incorporated in the calculus, if required, but it could be neglected in our experiments). We now suppose that protons are produced at the anode concomitantly with metallic cations. We shall now call *zone 1* the region of the electrolyte that is not yet perturbed by the dissolution of the anode, and *zone 2* the zone where impurities produced at the anode, and especially protons, can be found. The quantities in zone 2 (concentrations, speeds, etc.) will be labeled with a star. The two zones are separated by an invisible front which is described in detail in Ref. [18].

The question arises of what the concentration profiles in zone 2 are. Since protons are produced, the anode will produce fewer copper ions, so that the electroneutrality and the conservation of current will still be satisfied. If a positive step C_{H}^* of concentration is expected for the protons, then a negative step must be expected in the concentration of copper, so that the cation concentration is no longer C_c but C_c^* ($C_c^* < C_c$), and we must have $C_{\text{H}}^* + z_c C_c^* = z_a C_a^*$. The problem is that the protons do not migrate with the same speed as the copper ions: how can the system manage to maintain the electroneutrality, while the speeds $v_{\text{H}} = \mu_{\text{H}} E$ for the proton and $v_c = \mu_c E$ for the cation are very different ($v_c < v_{\text{H}}$)? In order to solve the problem we make the following hypothesis:

there exists a steady state on *both sides* of the invisible front. This is to say that while the concentrations are C_c and C_a and the field is E in zone 1, the concentrations in zone 2 are uniform with values (to be determined) C_{H}^* , C_c^* , and C_a^* and the field in zone 2 is E^* . The interface between the two zones is, in fact, a discontinuity in the concentrations and in the electric field.

This hypothesis is strongly supported by experiment: the dependence of the potential with time is linear in the two zones, and does not depend on the distances between electrodes [18]. The growth speed is almost constant in the two zones.

We now calculate the concentrations C_c^* and C_a^* and the field E^* as a function of the concentration C_{H}^* which is produced at the anode (which is an unknown data).

In zone 1, the conservation of current gives

$$E = \frac{J}{e(z_c \mu_c C_c + z_a \mu_a C_a)},$$

while in zone 2 we have

$$E^* = \frac{J}{e(z_c \mu_c C_c^* + z_a \mu_a C_a^* + \mu_{\text{H}} C_{\text{H}}^*)},$$

$$E^* = \frac{J}{e[z_a(\mu_c + \mu_a)C_a^* + (\mu_{\text{H}} - \mu_c)C_{\text{H}}^*]}.$$

Now, we cannot allow any accumulation of ions at the interface itself, because if ions would accumulate at the interface, there would be no way of hindering a leakage of the interface from the side of smaller field to the side of larger field, and then, there would be no steady state. We must then equate the rates of drifting in and out of the ions. This becomes for the anions, in the moving frame of the front

$$C_a^*(-\mu_a E^* - \mu_{\text{H}} E^*) = C_a(-\mu_a E - \mu_{\text{H}} E^*),$$

which gives

$$\frac{[(\mu_a + \mu_{\text{H}})C_a^* + \mu_{\text{H}} C_a]J}{z_a \mu_c C_c^* + z_a \mu_a C_a^* + (\mu_{\text{H}} - \mu_c)C_{\text{H}}^*} = \frac{\mu_a C_a J}{z_c \mu_c C_c + z_a \mu_a C_a}.$$

We finally have for C_a^*

$$C_a^* = \frac{\mu_{\text{H}} C_a (\mu_c z_c C_c + \mu_a z_a C_a) + \mu_a (\mu_{\text{H}} - \mu_c) C_a C_{\text{H}}^*}{(\mu_a + \mu_{\text{H}})(\mu_c z_c C_c + \mu_a z_a C_a) - \mu_a z_a C_a (\mu_c + \mu_a)}$$

$$= C_a \left[1 + \frac{\mu_a (\mu_{\text{H}} - \mu_c) C_a C_{\text{H}}^*}{\mu_{\text{H}} (\mu_c z_c C_c + \mu_a z_a C_a)} \right]$$

(remember that $z_c C_c = z_a C_a$) and, since $C_c^* = (z_a / z_c) C_a^* - (1/z_c) C_{\text{H}}^*$,

$$C_c^* = C_c \left[1 - \frac{\mu_c (\mu_{\text{H}} + \mu_a) C_{\text{H}}^* C_{\text{H}}^*}{\mu_{\text{H}} (\mu_c z_c C_c + \mu_a z_a C_a)} \right],$$

and for the field

$$E^* = \frac{J/ez_c C_c}{\mu_c + \mu_a + \frac{\mu_H(\mu_c + \mu_a) + \mu_a^2 + \mu_c^2 + \mu_a \mu_c}{\mu_H(\mu_c + \mu_a)} (\mu_H - \mu_c) \frac{C_H^*}{z_c C_c}} .$$

When considering a binary, symmetrical electrolyte with $C_a = C_c = C$, $z_a = z = z$, and $\mu_a = \mu_c = \mu$, we get

$$C_a^* = C + (\mu_H - \mu) C_H^* / 2z\mu_H$$

and consequently

$$C_c^* = C - (\mu_H + \mu) C_H^* / 2z\mu_H ,$$

$$E^* = J / [2z\mu C + (\mu_H - \mu^2 / \mu_H) C_H^*] e .$$

This form is more practical for the interpretation: since the mobility of the proton is larger than the mobility of the cation (generally copper or zinc), the field in zone 2 is smaller than in zone 1, thus the growth speed is decreased when the deposit grows in zone 2. Also the anion concentration is larger, and the cation concentration is smaller. The above equations give the actual values of the concentrations and of the field in zone 2. In principle, these equations allow one to actually *measure* the concentration of protons, by comparing the linear variation of the potential difference on both sides of the Hecker transition, or by measuring the growth speed, which is given by $\mu_a E^*$. Straightforward calculations lead to the following relation between C_H^* and the ratio $\alpha = E/E^*$, of the field in zone 1 over the field in zone 2,

$$C_H^* = z_c C_c \left[\frac{\alpha \mu_a - \mu_H}{\mu_a + \mu_H} - \frac{-\alpha \mu_c + \mu_H}{-\mu_c + \mu_H} \right] .$$

In the case shown in Fig. 12, the concentration of protons is found to be of the order of 10^{-2} mol ℓ^{-1} .

Furthermore, the ratio Π will be modified because of the presence in the bulk of a different kind of charge carrier. If we restrict ourselves to the case where the only charge carrier produced at the anode, apart from the metallic cation, is the proton, we can write the charge that has entered the deposit as

$$\int_0^T I dt = \int_0^{t^*} \sigma \frac{v}{\mu_a} S dt + \int_{t^*}^t \sigma^* \frac{v^*}{\mu_a} S dt ,$$

where t^* is the time at which the front meets the first protons coming from the anode, and t is the time at which it arrives at the other end. So

$$\int_0^T I dt = \frac{\sigma}{\mu_a} S L^* + \frac{\sigma^*}{\mu_a} S (L - L^*) ,$$

where L^* is the place at which the Hecker effect occurs. And the quantity Π^* which is actually measured, instead of the real copper ratio, is

$$\Pi^* = 1 + \frac{\mu_c}{\mu_a} + \left[1 - \frac{L^*}{L} \right] \frac{(\mu_H - \mu_c)(\mu_a + \mu_H)}{\mu_H(\mu_c + \mu_a)} \frac{C_H^*}{z_c C_c} .$$

Now, in this expression, L^* is known and the concentration profiles are known in both zones, as functions of the proton concentration. So, a value of C_H^* can be derived from the departure of Π^* from the value of Π . For example, in the same case where C_H^* was calculated from the change in the slope of $V(t)$, we find, from the independent measurement of Π^* , the value $C_H^* = 0.9 \times 10^{-2}$ mol ℓ^{-1} , which is in excellent agreement with the value derived from the change of slope. Still, one must keep in mind the fact that many sources of errors are certainly present, such as presence of other kinds of impurities, errors in the time at which the front is considered to have started, error in the time at which it is considered to have stopped, possible time delays when the deposit meets the step in proton concentration, and has to rearrange in order to keep on growing, and errors in C .

Also, it is not clear whether all the hydrogen is reduced when it arrives on the deposit, as is implicitly assumed in the above calculations. The situation is very far from equilibrium, and the structure of the surface is so complicated that it seems a formidable task to make a prediction of the quantity of protons which is reduced and the quantity of protons which remain in the rear zone of the deposit, with a corresponding balance of negative ions.

The dependence of Π^* on the current, especially in the case of copper acetate, is certainly due to an increased production of protons by the anode, when working with higher currents [20]. Experiments aiming at checking that the increase in Π^* can be related to a direct measurement of the *pH* are in progress.

VI. *IN SITU* MEASUREMENT OF THE POTENTIAL

In order to measure the potential of the solution in the vicinity of the tip of the branches, we have built a microprobe bearing ten copper wires per centimeter, touching the surface of the electrolyte, and recording the volts at their tips during the growth of the branches. Two runs with eight and seven microprobe wires are shown in Figs. 13 and 14.

The interpretation for the first figure is the following: the first flat zone gives the potential difference between the wire and the anode; as long as the front has not yet passed under the wire, this potential difference is the Ohmic potential drop due to the electrolyte between the wire and the anode. The experiment then tells that this potential difference is almost constant. This is in agree-

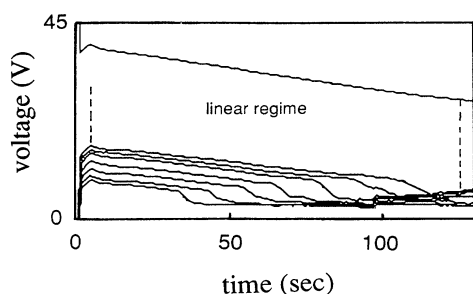


FIG. 13. Experimental recording of the potential drop between points in the solution and the anode. The upper measurement is made 5 mm away from the cathode and the lower one is made 7 mm away from the anode. Distance between anode and cathode is 2 mc. Concentration of copper sulfate: 10^{-2} mol ℓ^{-1} . The current is 2 mA and the thickness is 0.2 mm. As long as the deposit has not passed the probes, the potential difference is constant: the solution between the probes and the anode behaves as a constant resistor, its concentration is then almost constant.

ment with the expectation that the electrical equivalent of the solution, between a point in the bulk and the anode, remains identical, except for the tiny piling-up zone whose resistance is negligible and a possible slight decrease in resistance due to proton formation. The nearly vertical transition happens when the branches that advance in the solution pass near the wire. This transition occurs at different times for each wire since the wires are located at different places between the cathode and the anode (due to technical problems the spacings be-

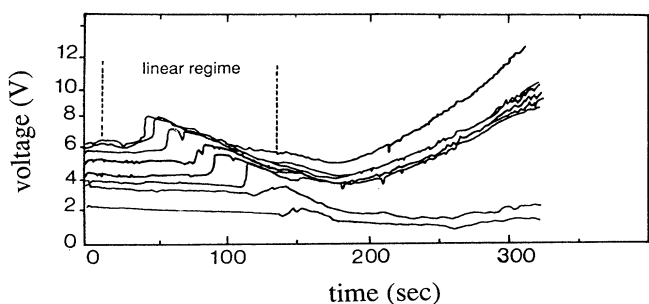


FIG. 14. Experimental recording of the potential difference between points in the solution and the cathode. The experimental conditions are 10^{-2} mol ℓ^{-1} , 3.5 mA. The potential decreases linearly while the branches of the deposit get closer to the probe (mind the scale which is different from that in Fig. 13). There is a clear potential drop at the tips. After the deposit has passed under the probe, the potential difference remains constant.

tween the wires were not exactly identical, so the different curves shown on Figs. 13 or 14 are not equally spaced), and are reached at different times by the branches of the deposit. Afterwards, a given wire records a potential difference that exhibits a linear decrease caused by the shrinking of the neutral zone between the tips and the anode. Since the neutral zone shrinks at a constant speed, so drops the potential. The very last zone shows the noisy regime that finally occurs. Meanwhile, anions and cations pile up at the anode, but these participate very little, as explained before, in the general conducting properties of the neutral zone.

The most interesting feature of this experiment is the drop of a few volts that is measured at the front. This means that there is indeed a discontinuity between the potential in the branches and the potential in the neutral region. This confirms the existence of a zone where the electric field is still large, near the tips of the branches. Since the distance between probes is 1 mm, we can derive from the data that the distance over which the potential falls is certainly smaller than $100 \mu\text{m}$. However, this potential drop looks very much like the potential drop expected on theoretical grounds in order to explain the growth of branches. Let us recall that following Ref. [14], we believe that the growth of the branches is needed in order to prevent the formation of a depleted zone where the field would otherwise be enormous. As it appears in Figs. 13 and 14, the formation of the depleted zone is efficiently hindered by the growth of the branches but there remains a sharp potential drop right at the front.

Moreover, the general outlook of these curves strongly suggests that the zone behind the wires is almost equipotential during the linear regime. This is very clear in Fig. 13 where the potential difference between the probes and the cathode is recorded. One expects that if the deposit were a perfect conductor, the potential difference would fall to zero as soon as the deposit reaches the probe. A sharp fall is indeed observed; however, the fall does not go to zero, thus revealing that the deposit is not a perfect conductor. We could estimate from several data the linear resistance of the filaments as being comprised between 300 and $3000 \Omega/\text{cm}$, so the resistance of the deposit is of the order of a few percent of the Ohmic zone of the solution. (Values of the resistance of the same order of magnitude, in the case of deposits grown with a supporting medium (paper), have been reported in Ref. [9(c)].) Some care must be taken in interpreting the data because several bubbles always occur right at the Hecker transition. These bubbles might be responsible in some cases for a malfunction of the probe.

The potential drop was found to vary with the applied electric field. A detailed study of this dependence will appear elsewhere. However, as we see in Fig. 15 that there is an increase of the potential drop with increasing applied current density. In our experiments, with a linear geometry and a constant current, the potential drop is then constant at the tips, thus providing a real steady state. In the experiments reported with a constant potential, and/or a circular geometry, the growth is never in a real steady state, not only because the current density

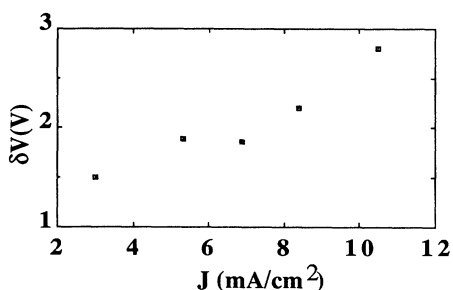


FIG. 15. Dependence of the potential drop on current density ($C=2 \times 10^{-2}$ mol ℓ^{-1}). There is an increase of the potential drop which shows that a steady state for the growth only exists when working with a constant current density. This is the case in parallel geometry and constant current.

varies, but also because the potential drop at the tips will depend on the size of the deposit.

VII. CONCLUSION

All the results that we have reported strongly demonstrate some new and some old assumptions on the dense-morphology regime of copper electrodeposition. These are as follows: after the initial stage during which the stable front is formed and until the branches arrive in the vicinity of the anode, the copper branches can be modeled as a flat continuous smooth area advancing into a solution of copper sulfate and repelling the anions in the zone free of deposit. We have proved that this

motion is due to the drift of the anions that forces the growth of the branches. This speed is monitored by the current density. Therefore the system selects the branching rate and the porosity of the deposit in order to satisfy the electrochemical conditions of the experiment: concentration, cell thickness, and other possible relevant parameters. At the tips of the branches a potential drop is found, which is the limiting value of a withstandable potential drop, beyond which branches form.

We have also shown that a moving front of different pH that advances in the solution towards the deposit is responsible for the existence of two zones where two different steady states occur, in which we give the actual values of the concentrations and of the field. These zones are separated by a propagating discontinuity surface that provokes the Hecker effect when arriving on the deposit, as it was already known.

This paper did not address the question of morphology on the microscopic level, nor the fractal character of the deposits grown at low current densities. Results on purely morphological themes are planned for presentation elsewhere.

ACKNOWLEDGMENTS

V. Fleury wishes to acknowledge fruitful discussions with Dr. M. Kolb. The experiments reported here have been supported by the Centre National d'Etudes Spatiales under Contract No. 89/1229. The Laboratoire de Physique de la Matière Condensée is "Unité Associée au Centre National de la Recherche Scientifique No. 1254."

- [1] M. Matsushita, M. Sano, Y. Hayakawa, H. Honjo, and Y. Sawada, *Phys. Rev. Lett.* **53**, 286 (1984).
- [2] D. Grier, E. Ben-Jacob, R. Clarke, and L. M. Sander, *Phys. Rev. Lett.* **56**, 1264 (1986).
- [3] Y. Sawada, A. Dougherty, and J. P. Gollub, *Phys. Lett.* **56**, 1260 (1986).
- [4] E. Ben-Jacob, G. Deutscher, P. Garik, N. D. Goldenfeld, and Y. Larea, *Phys. Rev. Lett.* **57**, 1903 (1986).
- [5] P. Garik, D. Barkey, E. Ben-Jacob, E. Bochner, N. Broxholm, B. Miller, B. Orr, and R. Zamir, *Phys. Rev. Lett.* **62**, 2703 (1989).
- [6] Nancy Hecker, David G. Grier, and L. M. Sander, in *Fractal Aspects of Materials*, edited by R. B. Laibowitz, B. B. Mandelbrot, and D. E. Passoja (MRS, Pittsburgh, 1985).
- [7] D. G. Grier, D. A. Kessler, and L. M. Sander, *Phys. Rev. Lett.* **59**, 2315 (1987).
- [8] F. Argoul, A. Arneodo, G. Grasseau, and H. L. Swinney, *Phys. Rev. Lett.* **61**, 2558 (1988).
- [9] (a) D. B. Hibbert and J. R. Melrose, *Phys. Rev. A* **38**, 1036 (1988); (b) J. R. Melrose, D. B. Hibbert, and R. C. Ball, *Phys. Rev. Lett.* **65**, 3009 (1990); (c) J. R. Melrose and D. B. Hibbert, *Phys. Rev. A* **40**, 1727 (1989).
- [10] G. L. M. K. S. Kahanda and M. Tomkiewicz, *J. Electrochem. Soc.* **136**, 1497 (1989) and references therein.
- [11] R. M. Brady and R. C. Ball, *Nature* **309**, 225 (1984).
- [12] T. A. Witten and L. M. Sander, *Phys. Rev. Lett.* **47**, 1400 (1981).
- [13] T. A. Witten and L. M. Sander, *Phys. Rev. B* **27**, 5686 (1983).
- [14] J.-N. Chazalviel, *Phys. Rev. A* **42**, 7355 (1990).
- [15] V. Fleury, J.-N. Chazalviel, M. Rosso, and B. Sapoval, *J. Electroanal. Chem.* **290**, 249 (1990).
- [16] J. O'M. Bockris and A. K. N. Reddy, *Modern Electrochemistry* (Plenum, New York, 1977), Vol. 1.
- [17] The morphological transition is easily seen on DM deposits because the eye distinguishes a line that is the envelope of transition points. They are as numerous as trees in the deposit, and thus often more than one per millimeter. When looking at "fractal" deposits one does not see the transition points very well because, as the pattern is fractal, branches only occur far apart from each other. However, a careful detailed viewing, which is generally not possible with the digitizing software, shows that morphological changes also occur in fractal deposition.
- [18] V. Fleury, M. Rosso, and J.-N. Chazalviel, *Phys. Rev. A* **43**, 6908 (1991); V. Fleury, J.-N. Chazalviel, M. Rosso, and B. Sapoval, in *Extended Abstracts of Congrès de Métallurgie de l'Institut National des Sciences et Techniques Nucléaires, Centre d'Etudes Nucléaires de Saclay, 1990* [*Ann. Chim.* **16**, 148 (1991)].
- [19] V. M. Castillo, R. D. Pochy, and L. Lam, in *Application of Statistical and Field Theory to Condensed Matter*, edited by A. R. Bishop (Plenum, New York, 1990).
- [20] In the case of a weak electrolyte, the dissociation equilibrium condition, which requires a certain value of the pH, should also be satisfied.